PROCESS DEVELOPMENT OF SILICON HETEROJUNCTION INTERDIGITATED BACK-CONTACTED (SHJ-IBC) SOLAR CELLS BONDED TO GLASS

Menglei Xu[1], Twan Bearda, Hariharsudan Sivaramakrishnan Radhakrishnan, Shashi Kiran Jonnak, Miha Filipič, Valerie Depauw, Kris Van Nieuwenhuysen, Yaser Abdulraheem[2], Maarten Debucquoy, Ivan Gordon, Jozef Szlufcik, Jef Poortmans[1,3]

IMEC, Leuven, Belgium
[1]Also with KU Leuven, Leuven, Belgium
[2]Kuwait University, Safat, Kuwait
[3]Also with Universiteit Hasselt, Hasselt, Belgium

ABSTRACT: In imec's i²-module concept, silicon heterojunction interdigitated back-contacted (SHJ-IBC) solar cells are fabricated on monocrystalline foils bonded to glass. The proposed technology allows for cell processing on thin wafers mechanically supported by the glass, increasing the yield of processing such thin wafers. A process sequence for SHJ-IBC cell fabrication that can be applied to bonded thin foils is described. We investigated and optimized individual process steps on thick wafers. Then the developed steps were integrated into a process flow to fabricate solar cells on wafers with different thicknesses and bonding agents. On wafers with a thickness of 190 µm, functional cells with efficiencies of 22.6% and 21.7% were made on freestanding and silicone bonded wafers, respectively. On thin wafers of 57 µm, our best SHJ-IBC cell on an EVA bonded wafer exhibits excellent V_{oc} of 740 mV and efficiency of 20.0%, which demonstrates the high potential of the i²-module concept.
Keywords: Amorphous Silicon, Heterojunction, Silicon Solar Cell, interdigitated back-contacted, Superstrate Processing

1 INTRODUCTION

The cost of silicon material accounts for approximately 61% of today's solar cell cost and 30% to 40% of the total c-Si solar module cost [1]. Hence, to reduce the silicon consumption, fabrication of solar cells on thin monocrystalline silicon foils is being studied by several groups [2-4].

Imec proposed the i²-module concept, which allows for large-scale module level processing of interdigitated back-contacted (IBC) solar cells on 40 µm thin silicon foils bonded to glass [5]. The glass delivers mechanical support to the thin foil and thus significantly reduces the foil breakage during cells processing. The choice for an IBC device allows to process the junction and the contacts after bonding. Certain constraints are imposed to the cell process mainly due to the bonding and the glass. For that reason, an a-Si:H heterojunction process is chosen for junction formation as that allows to keep the processing temperature low.

In this contribution, we report the recent progress in the process development of silicon heterojunction IBC (SHJ-IBC) solar cells. An integration process is presented, which is fully compatible with thin foils bonded to glass. Functional cells were fabricated on both freestanding and bonded n-type float zone (FZ) wafers with different thicknesses. Two different bonding adhesives, i.e., silicone and Ethylene Vinyl Acetate (EVA), are evaluated at cell level. The factors limiting the cell performance are identified and the main losses of the cells are discussed in detail.

2 RESULTS AND DISCUSSION

2.1 Integration process

All cells, with an area of 3.97 cm², were processed on 190 µm and 57 µm thick n-type FZ wafers (6 inch, <100>, 3Ω-cm).

The wafers were exposed to Sulfuric acid/Ozone mixture (SOM) and following HF:HCl:H_2O (2:5:93) solution for cleaning. Tetramethyl ammonium hydroxide (TMAH) based solution was used for thinning down and texturing of the wafers. As shown in Figure 1, the textured front side underwent PECVD a-Si:H passivation and SiN_x antireflection coating, followed by bonding to glass using EVA or silicone encapsulant. We have reported previously that plasma-silicone interaction during a-Si:H deposition has a detrimental impact on passivation quality [6]. Hence, silicone bonded wafers were treated with Ar plasma to form a more densely crosslinked layer by local modification of the exposed silicone surface [6]. Then the depositions of a-Si:H (i/n+) and a stack of SiO_x/a-Si:H were performed. This SiO_x layer is a sacrificial mask for subsequent lift-off process and the top a-Si:H layer is used to protect SiO_x during HF dip prior to a-Si:H (i/p+) deposition. Photolithography and wet etching were used to define the back surface field (BSF) area. The emitter was passivated by a-Si:H

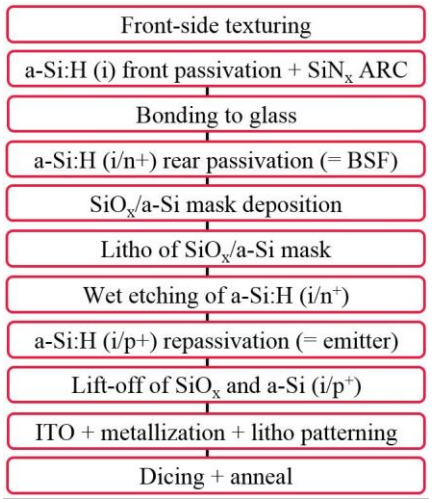

Figure 1: Integration process flow of SHJ-IBC cells on bonded substrate.

(i/p+) and patterned by self-alignment lift-off process, which was carried out in dilute HF. A stack of indium-doped tin-oxide (ITO) and Cu was deposited to form the rear side metal contact. Thermal annealing was applied to the finished cells in order to improve the contact behaviour. To investigate the influence of the presence of bongding agents and glass on the cell performance, identical cells were also fabricated on freestanding wafers without bonding to glass.

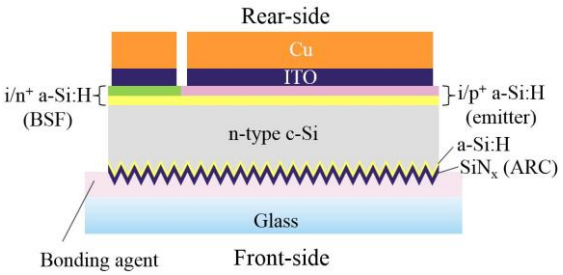

Figure 2: The cross-sections (not drawn to scale) of the bonded SHJ-IBC solar cells are depicted in the diagram.

2.2 Device results

The cell results are shown in Table I. For the best cells before anneal, we observe an improvement of $\Delta\eta$ = 0.5% on freestanding cells with respect to silicone bonded cells. This is due to an absolute increase ΔV_{oc} = 8 mV and ΔFF = 0.7%, but more significantly due to an increase ΔJ_{sc} = 1.1 mA/cm^2. Figure 3 compares the external quantum efficiency (EQE) of cells on freestanding wafers with that on silicone and EVA bonded wafers. The difference in EQE suggests that glass and silicone at the front side lead to additional reflectance and absorption losses for a wide range of wavelengths. Nevertheless, a high J_{sc} of 41.2 mA/cm^2 was still achieved on silicone bonded cells.

Table I: Best Cell results on freestanding and bonded wafers

Bonding Thickness	Anneal	J_{sc} (mA/cm^2)	V_{oc} (mV)	FF (%)	η (%)
freestanding 190 µm	before	42.3	735	69.7	21.5
	after	41.8	730	74.8	22.6
Silicone 190 µm	before	41.2	727	70.4	21.0
	after	40.8	734	73.1	21.7
EVA 190 µm	before	40.7	718	68.6	20.0
	after	39.9	724	71.6	20.7
EVA 57 µm	before	38.8	738	67.5	19.0
	after	38.6	740	71.7	20.0

For the cells on EVA bonded thick wafers, the best J_{sc} is 40.7 mA/cm^2 that is 0.5 mA/cm^2 lower than that of silicone bonded cells. As shown in Figure 3, this result can be attributed to the light absorption loss at short wavelength due to the UV blocker contained in EVA. And for the EVA bonded cells on 57 µm thin wafer, a J_{sc} of 38.8 mA/cm^2 was achieved, which is further limited by the light absorption loss at long wavelength.

The excellent V_{oc} of 734 mV and 740 mV were obtained on the silicone bonded and EVA bonded cells after anneal, respectively, similar to the V_{oc} of cells without bonding agent. It indicates that the impact of bonding agents on the surface passivation quality has been prevented. Such achievement has been made possible by several adaptations in the process:

- The new encapsulants silicone and EVA were selected to replace the previously used PV 6100 [7], because these alternative bonding agents were proven to be more resistant to chemicals and plasma treatments.
- An optimized curing/outgassing step reduces outgassing of bonding agents during a-Si:H deposition.
- The Ar plasma improves crosslinking of the silicone, and hence reduces the plasma-silicone interaction.
- The SiO_x hard mask (~680 nm) also covers the bonding agents during rear side process and thus further reduces the interaction of plasma /chemicals and bonding agents.
- Optimum a-Si:H deposition conditions were chosen for surface passivation in presence of different bonding agents.

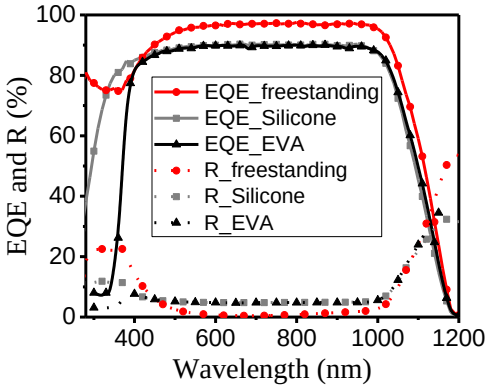

Figure 3: External quantum efficiency of a cell on freestanding wafer compared to that on bonded wafers. The thicknesses of the wafers are 190 µm.

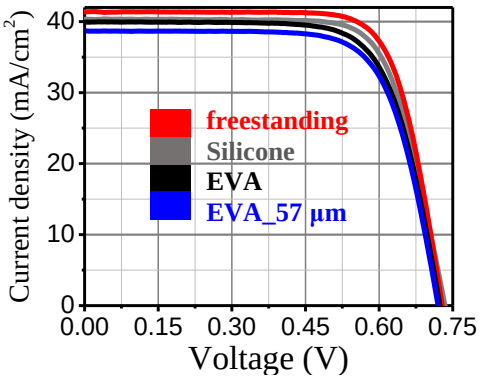

Figure 4: Light J-V curve of the best SHJ-IBC cells after anneal on freestanding and bonded wafers.

Table II: FF loss analysis of a cell on a freestanding wafer before and after anneal

Anneal	Cell parameters				FF loss analysis	
	R_s ($\Omega.cm^2$)	R_{sh} ($\Omega.cm^2$)	FF (%)	pFF (%)	ΔFF_{Rs} (% absolute)	ΔFF_{Rsh} (% absolute)
before	2.8	2.2×10^3	68.0	84.1	13.5	0.6
after	1.6	2.1×10^3	73.8	82.5	7.9	0.6

For all cells before annealing, the efficiencies are strongly limited by the relatively low FF (≤70.4%). Thermal anneals of the finished cells at temperatures below 200°C were performed under air ambient, which yielded a significant improvement in FF. For cells on freestanding wafers, the highest FF of 74.8% has been achieved after annealing at 150°C. A detailed FF loss analysis is shown in Table II [8]. The series resistance R_s was determined by the Bowden method at different light intensities [9]. The shunt resistance R_{sh} was determined by a linear fit of the dark I-V curve. The pseudo fill factor (pFF) was extracted from Suns-V_{oc} measurements. The absolute FF loss ΔFF_{Rs} was calculated to be 13.5%, while ΔFF_{Rsh} was only 0.6%. This reveals that the drop of the measured FF was primarily caused by series resistance. After annealing, R_s reduced significantly from 2.8 $\Omega.cm^2$ to 1.6 $\Omega.cm^2$, where corresponding ΔFF_{Rs} reduced from 13.5% to 7.9%.

3 CONCLUSION AND OUTLOOK

We presented an integration process for module-level processing of SHJ-IBC solar cells, which is compatible with thin silicon foils bonded to glass. Individual process steps have been investigated and optimized. To demonstrate the developed process, highly efficient cells on 190 µm and 57 µm thick wafers were fabricated. Issues limiting the cell performance were identified. Current development is the introduction of thin epitaxially grown wafers instead of thin FZ wafers [10]. Next steps will be directed towards improvement of fill factor and proces simplifications, including investigations and integration of lithography-free emitter patterning approach, dry etching of a-Si:H (already demonstrated in [11]) and selective depositon of a-Si:H to replace lift-off.

ACKNOWLEDGEMENTS

The authors gratefully acknowledge the financial support of imec's industrial affiliation program for Si-PV. This work was also partially funded by Kuwait Foundation for the Advancement of Sciences under project code: P115-15EE-01. The research leading to these results has received funding from the European Union's Seventh Programme for research, technological development and demonstration under grant agreements n° 609788 (Cheetah), and also funding from the European Union's Horizon 2020 research and innovation programme under the Marie Sklodowska-Curie grant agreement No 657270.

REFERENCES

[1] SEMI, International Technology Roadmap for Photovoltaic (ITRPV) (2016)
[2] J. Govaerts et al., Energy Procedia 77 (2015) 871
[3] S. Schoenfelder et al., Energy Procedia 38 (2013) 942
[4] L. Wang et al., IEEE J. Photovoltaics 4 (2014) 1397
[5] J. Govaerts et al., Sol. Energy Mater. Sol. Cells 113 (2013) 52
[6] S.N. Granata et al., Sol. Energy Mater. Sol. Cells 124 (2014) 48
[7] T. Bearda et al., 31st EUPVSEC (2015) p365
[8] A. Khanna et al., IEEE J. Photovoltaics 3 (2013) 1170
[9] S. Bowden et al., 17th EUPVSEC (2001) p1802
[10] K Van Nieuwenhuysen et al., 28th EUPVSEC (2012) p2471
[11] H. Sivaramakrishnan Radhakrishnan et al., 43rd IEEE PVSC (2016) conference proceedings